Estimation of a Geoid Section across the Kuroshio*

W. J. TEAGUE, Z. R. HALLOCK, AND G. A. JACOBS

Naval Research Laboratory, Stennis Space Center, Mississippi

14 March 1996 and 2 August 1996

ABSTRACT

An estimate of the geoid across the Kuroshio Extension at its separation point from Japan is calculated through an analysis of coincident sea surface measurements from inverted echo sounders (IESs) and Topex/Poseidon (T/P). The IESs were positioned along a T/P descending ground track in the vicinity of 35°N, 143°E. This geoid section can be used in conjunction with altimeter data to estimate total sea surface height. Thus, Kuroshio position, surface geostrophic velocity, and transport along the section can be continuously monitored.

1. Introduction

The satellite altimeter measures the distance between the satellite and the ocean surface. When combined with precise orbit determination, this provides a measurement of sea level (SL), the height of the ocean surface above the earth's reference ellipsoid. In the absence of currents and external forcing, SL coincides with the geopotential surface known as the geoid. The altimeter SL measurement is the sum of the geoid, which is constant in time, plus sea surface height departures (SSH) due to oceanographic features such as currents and tides. However, the spatial variations of the geoid are one to two orders of magnitude larger than SSH spatial variations. Thus, separation of the geoid from the mean SL is not possible from altimeter data alone. Without an accurate geoid from independent measurements, only temporal variations of SSH about mean SL are observable. Thus, the main focus of altimetry has traditionally been SSH variability.

A method used previously for estimation of the geoid consists of subtracting a mean SSH based on climatological in situ data, such as from the Levitus climatology (Levitus 1982) or the Generalized Digital Environmental Model (GDEM) (Teague et al. 1990), from the mean SL measured by the altimeter. However, the climatological mean SSH is not expected to be an accurate mean during the altimeter sampling time due to variations in ocean currents, which have longer periods than the altimeter sampling record. Thus, errors are expected to exist in the geoid derived through this method. Geoid errors produce a bias (not just random white noise errors) in the mean SSH and, therefore, fictitious geostrophic currents are inferred.

In situ sampling of the ocean dynamic height simultaneous with the altimeter sampling of SL can produce more realistic representations of the geoid for oceanographic purposes. Through airborne expendable bathythermograph surveys made simultaneously with altimeter measurements (Mitchell et al. 1990; Carnes et al. 1990), geoid accuracies are about 10 to 20 cm rms. However, very few samplings are available through these methods to reduce data noise. Thus, long time series of both in situ and altimeter sampling are necessary.

Here, we calculate the geoid beneath a section of one Topex/Poseidon (T/P) ground track with T/P altimeter and in situ inverted echo sounder (IES) data. The two datasets are concurrent so that the mean observed by each is evaluated over the same time period. Both datasets cover about 2 years and the T/P satellite has a repeat period of about 10 days. Thus, about 70 measurements of the geoid are made to reduce data noise to an error generally better than 3 cm rms. The rms error of the SSH from this geoid using T/P altimetry is about 8 cm. It is essential that long time period in situ measurements be combined with altimeter data where possible so that SSH may be directly observed from the altimeter system.

2. Measurements

The IES measurements are part of the Kuroshio Extension Regional Experiment (KERE) (Mitchell 1990). This program was initiated in 1991 and consisted of T/P altimetry (Benada 1993), extensive basin-scale numerical modeling (Mitchell et al. 1996; Jacobs et al. 1996; Hurlburt et al. 1996), and a regional in situ observational program. A main objective of the latter was to monitor the Kuroshio Extension near the separation point to determine variability levels and relation to the deep flows. The KERE field program consisted of intensive mea-

*Naval Research Laboratory–Stennis Space Center Contribution Number JA/7332-96-0009.

Corresponding author address: Mr. William J. Teague, Naval Research Laboratory, Stennis Space Center, MS 39529-5004.

Unauthenticated | Downloaded 07/20/24 03:15 AM UTC

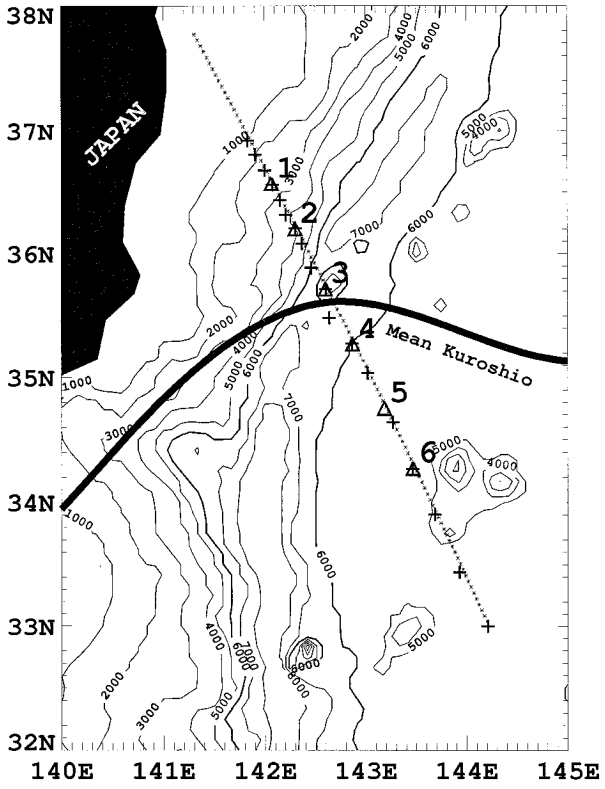

FIG. 1. IES/PG sites are indicated by triangles, Topex/Poseidon measurements by asterisks, and CTD stations by plus signs along the KERE section. The 6000-m depth contours (bold) indicate the boundaries of the Japan trench. The Kashima 1 seamount is located beneath the section at about 35.7°N. Bathymetry is from ETOPO 5 (NOAA 1986), a 5′ latitude by 5′ longitude worldwide gridded database, and generally reflects the actual depths measured when collecting these data.

surements along a section of a T/P groundtrack (henceforth referred to as the KERE section) across the Kuroshio Extension near 35°N, 143°E (Fig. 1). The data include currents measured by moored current meters at various depths, thermocline depths and pressures measured by inverted echo sounders with pressure gauges (Teague and Hallock 1995), and detailed hydrographic measurements. KERE hydrography is reported on in detail in Teague et al. (1993, 1994) and in Shiller et al. (1996), current measurements by Hallock and Teague (1995, 1996), and IES observations compared with T/P altimetry by Teague et al. (1995).

The in situ dataset spans July 1992 to June 1994 and extends from about 37°N, 142°E to 33°N, 144°E along a T/P descending groundtrack (Fig. 1). The KERE section begins near the shelf break just east of Honshu, Japan, extending southeastward across the southern part of the Japan trench. The water depth at the northern end of the KERE section is about 1000 m. Near its center, the KERE section crosses the Japan trench with depths greater than 7000 m. Within the Japan trench beneath the KERE section is the Kashima 1 seamount, which rises to about 4000-m depth.

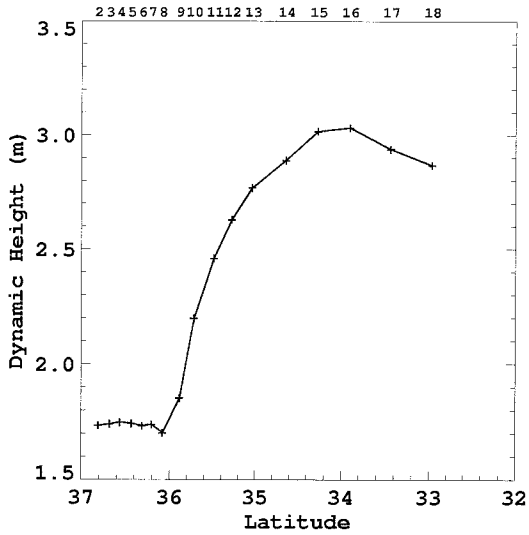

FIG. 2. Dynamic height referenced to 2000 m for the KERE section. CTD station locations are indicated by plus signs.

Six IES/PGs were positioned along the section. IES/PG spacing ranged from 40 to 60 km. The position of the Kashima 1 seamount was advantageous for placement of one of the IES/PGs. A conductivity–temperature–depth (CTD) survey also was made along this T/P groundtrack in July 1992 (Teague et al. 1993). The CTD spacing along the section telescoped from about 15 km at the northern end of the section to about 50 km on the southern end. The north wall of the Kuroshio was located near 35.8°N in the vicinity of the Kashima 1 seamount at the time of the CTD section.

A Neil Brown Mark III CTD was used to collect 18 closely spaced CTD/hydrographic stations from 8 to 23 July 1992 (Teague et al. 1993, 1994). The Kuroshio north wall, indicated from the temperature section by a sharp downward slope in the isotherms, was at approximately 35.9°N. The dynamic height cross-stream profile computed with respect to a 2000-m zero-velocity reference level is shown in Fig. 2 and corresponds to a maximum speed in the Kuroshio in excess of 170 cm s^{-1}. Dynamic height changes by about 1.3 m across the Kuroshio and has a maximum gradient of approximately 1.5 cm km^{-1}.

Topex/Poseidon was launched 10 August 1992 as a joint effort by National Aeronautics and Space Administration (NASA) and the French Space Agency, Centre National d'Etudes Spatiales (CNES), for studying global ocean circulation (Fu et al. 1994). The T/P mission is also coordinated with the World Ocean Circulation Experiment (WOCE) and the Tropical Ocean and Global Atmosphere program (TOGA). T/P data utilized in this study begin in late September 1992. The T/P data are obtained from the Geophysical Data Records (GDRs) processed at the Physical Oceanography Distributed Active Archive Center (PODAAC) at the Jet Propulsion Laboratory. T/P has a repeat period of 9.92 days and an equatorial cross-track separation of 315 km. T/P data are corrected for the effects

Unauthenticated | Downloaded 07/20/24 03:15 AM UTC

TABLE 1. Geographical positions of the IES/PGs and their distances to the closest Topex/Poseidon data.

IES/PG sites	1	2	3	4	5	6
Latitude (°N)	36.567	36.198	35.718	35.267	34.750	34.270
Longitude (°E)	142.067	142.300	142.598	142.868	143.183	143.467
Distance to Topex (km)	1.58	1.57	2.40	2.11	2.02	3.71

of wet troposphere from an onboard water vapor radiometer, dry troposphere, ionosphere from the dual-frequency altimeter, inverse barometer, and electromagnetic bias. The ionospheric correction is smoothed using a Gaussian filter with a rolloff of about 100 km along track. Tidal contamination is removed using the Cartwright and Ray (1991) tide model. The height data are interpolated along track to a reference ground track produced at the Colorado Center for Astrodynamics Research, resulting in about 7-km spacing.

IES/PG records are processed as described by Hallock et al. (1989). Briefly, hourly data series are low-pass filtered (half-amplitude at 40 h). Acoustic travel time and bottom pressure anomaly are converted to baroclinic ($H_{\rm bcl}$) and barotropic ($H_{\rm btr}$) components of sea surface height anomaly:

$$H'_{\rm bcl} = D'/g, \tag{1}$$

$$H'_{\rm btr} = P'_b/g\rho_b, \tag{2}$$

and dynamic height anomaly (temporal) is given by

$$D' = B\tau', \tag{3}$$

where g is the gravitational constant, P'_b is the bottom pressure anomaly, ρ_b is the density near the bottom, B is a regression coefficient based on hydrography in the region (Hallock 1987), and τ' is the acoustic travel time anomaly between the sea surface and bottom. The regression coefficient B, calculated with travel times inferred from the CTD observations and historical temperature and salinity data (Levitus 1982), is -4.35 ± 0.05 dynamic centimeters per millisecond. The error in B is primarily affected by near-surface temperature–salinity variability. In addition, there is a seasonal bias in B that is related to seasonal heating and cooling of near-surface waters. This effect is discussed by Teague et al. (1994). Statistical uncertainties dominate measurement error. Similar error statistics were found for the Gulf Stream and are fully discussed by Hallock et al. (1989). The total anomaly of SSH is given by

$$H'_{\rm IES} = H'_{\rm bcl} + H'_{\rm btr}. \tag{4}$$

Some of the pressure-gauge data contain unmodeled long-period drifts, a ubiquitous problem with this type of pressure sensor (Fields and Watts 1991), which can result in errors in the calculation of $H'_{\rm IES}$. Pressure records were acceptable at sites 3 and 5 after removing drifts modeled by exponential trends. Their rms variabilities were calculated using the 1-h resolution data. Average rms values using IES/PG data at sites 3 and 5 were, respectively, $\langle H_{\rm btr}\rangle = 0.041$ m, $\langle H_{\rm bcl}\rangle = 0.257$ m, and $\langle H_{\rm IES}\rangle = 0.262$ m. Here $\langle H_{\rm IES}\rangle$ is clearly dominated by $H_{\rm bcl}$. The ratio $\langle H_{\rm btr}\rangle$ / $\langle H_{\rm IES}\rangle$ is 0.16 and compares well with estimates by Hall (1989), which indicate that the barotropic component of mean SSH of the Kuroshio Extension represents about 19% of the total SSH variability. This ratio is about half the ratio (0.33) found for the Gulf Stream region by Hallock et al. (1989). Total amplitudes of $H_{\rm bcl}$ range over 1 m in the Kuroshio region. Thus, it is reasonable to estimate $H_{\rm IES}$ from $H_{\rm bcl}$ in this region. Calculations of $H_{\rm IES}$ made in this paper are based on $H_{\rm bcl}$ since the pressure records were problematic.

Expendable bathythermograph (XBT) observations were made at IES sites during deployment and are used to estimate total baroclinic SSH at those times, which we denote as $H_{\rm bcl}(0)$. We then calculate time series of $H_{\rm bcl}$ from $H'_{\rm bcl}$ as follows:

$$H_{\rm bcl} = \overline{H}_{\rm bcl} + H'_{\rm bcl}, \tag{5}$$

where

$$\overline{H}_{\rm bcl} = H_{\rm bcl}(0) - H'_{\rm bcl}(0). \tag{6}$$

Total $H_{\rm bcl}$ (rather then the temporal anomaly $H'_{\rm bcl}$) is needed to combine with T/P derived SL for geoid estimation.

3. Geoid estimation

In the present paper, $H_{\rm IES}$ at each IES site is calculated for almost coincident SL from T/P. Distances from the IES sites to the T/P ground points ranged from 1.5 to 3.7 km (Table 1), while the time differences between the measurements were always less than one-half hour.

The primary source of error in $H_{\rm IES}$ is in the conversion of IES acoustic travel times to dynamic heights. This error is about 7 cm rms for the Gulf Stream region (Hallock 1987) and is similar, 5 cm, for the Kuroshio region. Error variance is caused mainly by temperature and salinity variations in the upper 200 m of the water column. Analysis of the pressure records reveals that an error of up to 4 cm rms can occur by not including the barotropic contribution $H_{\rm btr}$ in $H_{\rm IES}$ calculations. Thus, the total rms error in IES SSH is about 6.4 cm. The error of altimeter measurements is estimated to be 4.8 cm rms (Fu et al. 1994). Errors due to the small (1–3 km, see Table 1) mismatch in the T/P and IES geographical positions can be about 2 cm rms due to the high spatial gradient in SSH in the vicinity of the Kuroshio or eddies. Errors caused by a maximum time offset of one-half hour are negligible for the calculations since the T/P and IES data have been detided. Maximum error estimated by the root sum square of the above errors is 8.2 cm.

Unauthenticated | Downloaded 07/20/24 03:15 AM UTC

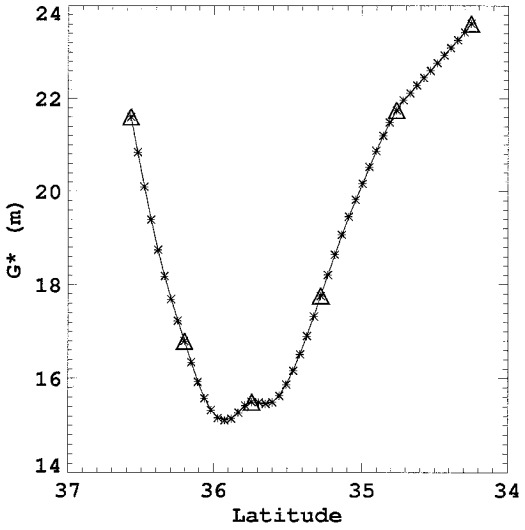

FIG. 3. Geoid estimation at Topex/Poseidon ground points (asterisks) and IES/PG sites (triangles).

A geoid section can be estimated along the T/P track for each repeat pass, *i*. The sea level SL measured by the altimeter is the sum of the geoid and the SSH:

$$\mathrm{SL}_i = G + \mathrm{SSH}_i, \tag{7}$$

where G is the geoid height and SSH_i is due to ocean currents. The SSH height approximated from the IES data, described in section 2, is

$$H_{\mathrm{IES}} = H'_{\mathrm{bcl}} + \overline{H}_{\mathrm{bcl}}. \tag{8}$$

A single geoid estimate, G_i is thus

$$G_i = \mathrm{SL}_i - H_{\mathrm{IES}i}. \tag{9}$$

The best geoid estimate, G^* at the IES position is

$$G^* = \frac{1}{N}\sum_{i=0}^{N} G_i = \overline{\mathrm{SL}} - \overline{H}_{\mathrm{IES}}, \tag{10}$$

where N is the number of T/P repeat passes (70 were used), $\overline{\mathrm{SL}}$ is the mean sea level derived from N passes, and $\overline{H}_{\mathrm{IES}}$ is the corresponding mean height from the IES data. The standard error E in the geoid estimate is

$$E = \frac{\sigma(G^*)}{N^{1/2}}, \tag{11}$$

where σ is the standard deviation. Here $\overline{H}_{\mathrm{IES}}$ can be approximated along track by interpolation thereby forming G estimates at each T/P ground point between IES sites.

The estimated geoid along the KERE section is shown in Fig. 3 and numerical values of the geoid with positions are given in Table 2. The geoid reflects the local topography of the Japan trench, and the bump near 35.75°N corresponds to Kashima 1 seamount. The gravimetric geoid supplied on the T/P GDR (Callahan 1993) misses the seamount entirely but has a somewhat similar shape to our estimated geoid. However, geostrophic velocities calculated with our estimated geoid are reasonable (from about 0 to 1 m s^{-1}), while velocities calculated with the GDR geoid are not realistic (from about -4 to 5 m s^{-1}).

An SSH profile can be calculated using T/P data along this geoid section. This profile can be used to provide a time series of Kuroshio along-track location and cross-track geostrophic speed. A times series of SSH along the KERE section is shown for the time period of Oc-

TABLE 2. Estimated geoid G^* and error E derived from Topex/Poseidon height data ($\overline{\mathrm{SL}}$) and IES height data ($\overline{H}_{\mathrm{IES}}$) over a 2-yr period. Note, for IES 6 (at 34.252°N) data were available only for the first year.

Lat. (°N)	Long. (°E)	$\overline{\mathrm{SL}}$ (m)	$\overline{H}_{\mathrm{IES}}$ (m)	G^* (m)	E (m)
36.571	142.084	23.412	1.807	21.604	0.019
36.525	142.114	22.648	1.807	20.841	
36.479	142.143	21.905	1.807	20.099	
36.433	142.172	21.200	1.807	19.393	
36.386	142.201	20.553	1.806	18.746	
36.340	142.230	19.990	1.806	18.184	
36.294	142.259	19.495	1.806	17.689	
36.248	142.288	19.035	1.806	17.230	
36.202	142.317	18.601	1.805	16.795	0.018
36.155	142.346	18.184	1.839	16.344	
36.109	142.375	17.802	1.873	15.930	
36.063	142.404	17.483	1.906	15.577	
36.017	142.433	17.266	1.940	15.327	
35.970	142.462	17.137	1.973	15.163	
35.924	142.490	17.120	2.007	15.113	
35.878	142.519	17.188	2.041	15.147	
35.831	142.548	17.346	2.074	15.272	
35.785	142.576	17.531	2.108	15.423	
35.739	142.605	17.640	2.141	15.499	0.023
35.692	142.634	17.653	2.165	15.488	
35.646	142.662	17.650	2.188	15.462	
35.600	142.691	17.704	2.212	15.492	
35.553	142.719	17.865	2.235	15.630	
35.507	142.748	18.126	2.258	15.867	
35.461	142.776	18.443	2.282	16.161	
35.414	142.804	18.817	2.305	16.512	
35.368	142.833	19.230	2.329	16.901	
35.322	142.861	19.670	2.352	17.318	
35.275	142.889	20.132	2.375	17.757	0.023
35.229	142.917	20.603	2.393	18.209	
35.182	142.945	21.055	2.411	18.644	
35.136	142.974	21.496	2.429	19.067	
35.089	143.002	21.907	2.447	19.460	
35.043	143.030	22.286	2.465	19.821	
34.997	143.058	22.653	2.483	20.170	
34.950	143.086	23.028	2.501	20.527	
34.904	143.114	23.393	2.518	20.874	
34.857	143.142	23.738	2.536	21.201	
34.811	143.169	24.044	2.554	21.490	
34.764	143.197	24.322	2.572	21.750	0.030
34.718	143.225	24.568	2.602	21.966	
34.671	143.253	24.753	2.631	22.122	
34.625	143.281	24.947	2.660	22.287	
34.578	143.308	25.139	2.689	22.450	
34.531	143.336	25.322	2.719	22.604	
34.485	143.364	25.515	2.748	22.767	
34.438	143.391	25.711	2.777	22.934	
34.392	143.419	25.901	2.807	23.095	
34.345	143.446	26.095	2.836	23.259	
34.299	143.474	26.296	2.865	23.431	
34.252	143.501	26.510	2.895	23.615	0.025

Unauthenticated | Downloaded 07/20/24 03:15 AM UTC

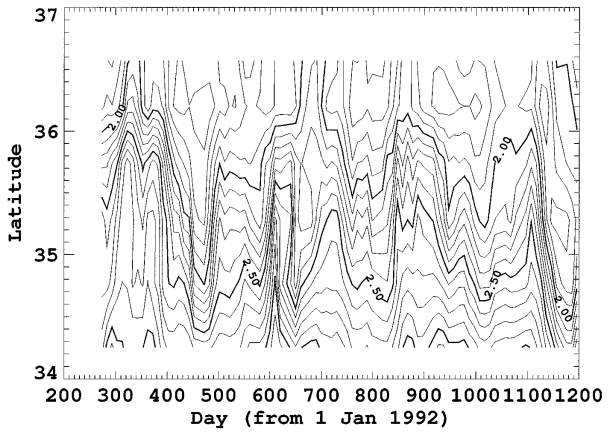

FIG. 4. A time series of sea surface height contours (m) along the KERE section computed from Topex/Poseidon data and the IES-derived geoid. The 2.2 contour line indicates the approximate location of the Kuroshio surface current axis.

tober 1992 through the end of 1995 in Fig. 4. The north wall of the Kuroshio is approximately tracked by the 2.2-m contour line. Large southward excursions of the Kuroshio are found to occur near days 470 and 1180 (Julian days 105 and 85, respectively).

4. Conclusions

The geoid provided in Table 2 for the T/P track along the KERE section has been estimated to an accuracy generally better than 8 cm rms. The maximum standard error in the geoid estimate is 3 cm. SSH can be estimated for all T/P passes along the KERE section by subtracting G^* from T/P-derived SL. Hence, T/P data, along this geoid arc segment, can provide good estimates of Kuroshio position and geostrophic speed. Observations such as these provide boundary conditions for numerical modeling and nowcasts of the Kuroshio.

Acknowledgments. The leadership of Jimmy Mitchell to the KERE project was invaluable. Thanks are extended to Steve Sova of NRL who prepared the IES/PGs and played a major role in their deployment and recovery and to Mark Hulburt of NRL who assisted. We appreciate the assistance given by the officers and the crew of the *Moana Wave* during the field operations. This work was supported by the Office of Naval Research as part of the Basic Research Project ''Kuroshio Extension Regional Experiment'' under Program Element 601135N.

REFERENCES

Benada, R., 1993: Merged GDR (TOPEX/POSEIDON) Users Handbook. Rep. JPL D-11007. Jet Propulsion Laboratory, 133 pp.

Callahan, P. S., 1994: TOPEX/POSEIDON Project GDR Users Handbook. Rep. JPL D-8944. Jet Propulsion Laboratory, 84 pp.

Carnes, M. R., J. L. Mitchell, and P. W. deWitt, 1990: Synthetic temperature profiles derived from Geosat altimetry: Comparisons with air-dropped expendable bathythermograph profiles. *J. Geophys. Res.*, **95,** 17 979–17 992.

Cartwright, D. E., and R. D. Ray, 1991: Energetics of global ocean tides from Geosat altimetry. *J. Geophys. Res.*, **96,** 16 897–16 912.

Fields, E., and D. R. Watts, 1991: The SYNOP Experiment: Inverted echo sounder data report for June 1989 to September 1990. GSO-Tech. Rep. 91-2, 255 pp. [Available from Graduate School of Oceanography, University of Rhode Island, Narragansett, RI 02882-1197.]

Fu, L.-L., E. J. Christensen, C. A. Yamarone Jr., M. Lefebvre, Y. Menard, M. Dorrer, and P. Escudier, 1994: TOPEX/POSEIDON mission overview. *J. Geophys. Res.*, **99,** 24 369–24 381.

Hall, M. M., 1989: Velocity and transport structure of the Kuroshio extension at 35°N, 152°E. *J. Geophys. Res.*, **94,** 14 445–14 459.

Hallock, Z. R., 1987: Regional characteristics for interpreting inverted echo sounder observations. *J. Atmos. Oceanic Technol.*, **4,** 298–304.

——, and W. J. Teague, 1995: Current meter observations during the Kuroshio Extension Regional Experiment. NRL Rep. MR/7332-95-7592, 119 pp. [Available from Naval Research Laboratory, Stennis Space Center, MS 39529-5004.]

——, and ——, 1996: Evidence for a North Pacific deep western boundary current. *J. Geophys. Res.*, **101,** 6617–6624.

——, J. L. Mitchell, and J. D. Thompson, 1989: Sea surface topographic variability near the New England seamounts: An intercomparison among in situ observations, numerical simulations, and Geosat altimetry from the Regional Energetics Experiment. *J. Geophys. Res.*, **94,** 8021–8028.

Hurlburt, H. E., A. J. Wallcraft, W. J. Schmitz Jr., P. J. Hogan, and E. J. Metzger, 1996: Dynamics of the Kuroshio/Oyashio current system using eddy-resolving models of the North Pacific Ocean. *J. Geophys. Res.*, **101,** 941–976.

Jacobs, G. A., W. J. Teague, J. L. Mitchell, and H. E. Hurlburt, 1996: An examination of the North Pacific Ocean in the spectral domain using Geosat altimeter data and a numerical ocean model. *J. Geophys. Res.*, **101,** 1025–1044.

Levitus, S., 1982: *Climatological Atlas of the World Ocean.* NOAA Prof. Paper 13, U.S. Govt. Printing Office, 173 pp.

Mitchell, J. L., 1990: Plans for the Kuroshio Extension regional experiment. NOARL Tech. Note 016:321:90, 34 pp. [Available from Naval Research Laboratory, Stennis Space Center, MS 39529-5004.]

——, W. J. Teague, G. A. Jacobs, and H. E. Hurlburt, 1996: Kuroshio extension dynamics from satellite altimetry and a model simulation. *J. Geophys. Res.*, **101,** 1045–1058.

NOAA, 1986: ETOPO 5 digital relief of the surface of the earth. Data Announcement 86-MGG-07, 2 pp. [Available from National Geophysical Data Center, Washington, DC 20233.]

Shiller, A. M., W. J. Teague, and Z. R. Hallock, 1996: Deep water properties near 35°N, 143°E observed during the Kuroshio Extension Regional Experiment. *J. Geophys. Res.*, **101,** 16 695–16 702.

Teague, W. J., and Z. R. Hallock, 1995: Inverted echo sounder observations during the Kuroshio Extension Regional Experiment. NRL Rep. MR/7332-95-7591, 61 pp. [Available from Naval Research Laboratory, Stennis Space Center, MS 39529-5004.]

——, M. J. Carron, and P. J. Hogan, 1990: A comparison between the generalized digital environmental model and Levitus climatologies. *J. Geophys. Res.*, **95,** 7167–7183.

——, Z. R. Hallock, J. M. Dastugue, and A. M. Shiller, 1993: Kuroshio Extension Regional Experiment hydrographic data: Summer 1992. NRL Rep. MR/7332-93-7050, 68 pp. [Available from Naval Research Laboratory, Stennis Space Center, MS 39529-5004.]

——, A. M. Shiller, and Z. R. Hallock, 1994: Hydrographic section across the Kuroshio near 35°N, 143°E. *J. Geophys. Res.*, **99,** 7639–7650.

——, ——, G. A. Jacobs, and J. L. Mitchell, 1995: Kuroshio Sea surface height fluctuations observed simultaneously with inverted echo sounders and TOPEX/POSEIDON. *J. Geophys. Res.*, **100,** 24 987–24 994.

Unauthenticated | Downloaded 07/20/24 03:15 AM UTC